TLR2-mediated leukocyte trafficking to the developing brain

Amin Mottahedin, Peter Lawrence Phillip Smith,* Henrik Hagberg,[†,‡] C. Joakim Ek,*[,1] and Carina Mallard*[,1,2]*

*Department of Physiology, Institute of Neuroscience and Physiology, and [‡]Perinatal Center, Department of Obstetrics and Gynecology, Sahlgrenska Academy, University of Gothenburg, Gothenburg, Sweden; and [†]Centre for the Developing Brain, Division of Imaging Sciences and Biomedical Engineering, King's College London, King's Health Partners, St. Thomas' Hospital, London, United Kingdom

RECEIVED DECEMBER 22, 2015; REVISED JUNE 23, 2016; ACCEPTED JULY 17, 2016. DOI: 10.1189/jlb.3A1215-568R

ABSTRACT

Inflammation is a significant risk factor for brain injury in the perinatal period. In this study, we tested the hypothesis that activation of peripheral TLR induces inflammation in the brain, including leukocyte trafficking. Postnatal day 8 mice were injected intraperitoneally with a TLR1/2 (Pam3CSK4, P3C), TLR2/6 (FSL-1) or TLR4 (LPS) agonist, and the peripheral and central cytokine and chemokine response was determined. Infiltration of immune cells to the CSF and brain was examined by flow cytometry, and brain permeability was investigated by radioactively labeled sucrose. We report that peripheral administration of P3C to neonatal mice induces significant influx of leukocytes, mainly neutrophils and monocytes, to the CSF and brain. Infiltration of leukocytes was TLR2 and MyD88 dependent, but largely absent after administration of LPS or FSL-1. PC3-mediated accumulation of immune cells in the brain was observed in classic CNS-leukocyte gateways, the subarachnoid space and choroid plexus, as well as in the median eminence. Although P3C and LPS induced a similar degree of peripheral inflammatory responses, P3C provoked a distinct brain chemokine response and increased permeability, in particular, of the blood-CSF barrier. Collectively, our results do not support the hypothesis that TLR activation, in general, induces immune cell infiltration to the brain. Instead, we have discovered a specific TLR2-mediated mechanism of CNS inflammation and leukocyte invasion into the neonatal brain. This interaction between peripheral and central immune responses is to a large extent via the blood-CSF barrier. *J. Leukoc. Biol.* 100: 000–000; 2016.

Introduction

Inflammation is increasingly understood to be an important risk factor for neonatal brain injury and subsequent neurologic syndromes, such as cerebral palsy [1, 2]. Proinflammatory cytokines are elevated in the CSF of asphyxiated term infants, and the level of inflammatory response reflects the degree of hypoxic-ischemic encephalopathy [3]. Cytokines are also elevated in newborns with severe intraventricular hemorrhage and in the brains of neonates with white matter injury [4]. Under physiologic conditions, the CNS is protected from blood-borne pathogens and immune cells by a physical BBB, which consists of tight junctions between brain endothelial cells. In a similar fashion, immune factors and circulating cells have limited entry into the CSF by an epithelial cell barrier at the choroid plexus [5]. These barriers are present and functioning from an early age [6, 7]. Increased permeability of the BBB in pathologic situations has been associated with brain injury [8, 9]; however, the degree of interaction between peripheral and central immune responses via the BCSFB and the mechanisms that underlie such communication remain, to a large extent, enigmatic.

The TLR subfamily of pattern recognition receptors are a well-characterized component of the innate immune system that detects pathogen- and damage-associated molecular patterns and initiate inflammatory responses [10]. We have previously shown that systemic administration of TLR3 and TLR4 agonists to newborn mice sensitize the brain to subsequent hypoxic-ischemic brain injury [11, 12] and the TLR2-deficient mice are protected from neonatal hypoxia-ischemia [13]. Furthermore, repeated systemic administration of the TLR1/2 agonist P3C impairs brain development in neonatal mice [14]. In adult mice, intrathecal injection of P3C causes neural loss and CSF pleocytosis [15]. Similarly, we have noted increased number of leukocytes in CSF in neonatal mice after systemic P3C administration [16]. However, the systemic inflammatory response initiated in response to TLR2 activation in newborns has not been fully profiled, and its effect on the developing CNS remains largely unknown.

Abbreviations: BBB = blood-brain barrier, BCSFB = blood-cerebrospinal fluid barrier, CSF = cerebrospinal fluid, EGFP = enhanced GFP, FSL-1 = fibroblast-stimulating lipopeptide 1, KO = knockout, P3C = PAM3CSK4 (palmitoyl-3-cysteine-serine-lysine-4), PND = postnatal day

The online version of this paper, found at www.jleukbio.org, includes supplemental information.

1. These authors contributed equally to this work.

2. Correspondence: Institute of Neuroscience and Physiology, Sahlgrenska Academy, University of Gothenburg, Box 432, 40530 Gothenburg, Sweden. E-mail: carina.mallard@neuro.gu.se

Here, we report for the first time, to our knowledge, on the systemic and cerebral inflammatory response, including cellular characteristics, to TLR2 activation in neonatal mice. We discovered TLR2- and MyD88-dependent leukocyte infiltration into the CSF and brain after systemic administration of P3C. In contrast, administration of TLR4 agonist, LPS, or TLR2/6 agonist, FSL-1, did not result in cell trafficking into the CSF.

MATERIALS AND METHODS

Animals

C57Bl/6J mice were purchased from Charles River Laboratories (Wilmington, MA, USA). TLR2 KO (B6.129-Tlr2tm1Kir/J) and MyD88 KO mice (B6.129P2 (SJL)-Myd88tm1.1Defr/J) were purchased from The Jackson Laboratory (Bar Harbor, ME, USA). *Lys*-EGFP-*ki* mice were obtained from Dr. Tomas Graf, Autonomous University of Barcelona (Barcelona, Spain). All transgenic animals were maintained on a C57BL/6J background and were housed and bred at the Laboratory for Experimental Biomedicine, University of Gothenburg, with ad libitum access to food and water on a 12-h light-dark cycle. Animal protocols were approved by the Gothenburg Animal Ethics Committee.

Experimental procedures

Eight-day-old mice (PND8) were injected intraperitoneally with either the TLR1/2 ligand P3C (Invivogen, Toulouse, France), the TLR4 ligand LPS (Serotype 055:B5, ultra-pure; List Biologic Laboratory, Campbell, CA, USA), or the TLR2/6 agonist FSL-1 (Invivogen). Dosages were 5 mg/kg or 1 mg/kg for P3C, 1 mg/kg or 0.3 mg/kg for LPS, and 0.3 mg/kg for FSL-1, and all were based on previous studies [4, 17]. Injection volume was 10 μl/g body weight. In one experiment, adult mice were injected intraperitoneally with 1 mg/kg P3C.

CSF collection and leukocyte count

Pups were killed at various time points after agonist administration by injection of an overdose of sodium thiopental followed by an incision in the heart. CSF (3–5 μl) was collected from the cisterna magna by using a fine glass capillary. CSF samples were discarded if any trace of blood contamination was observed. Samples were stained with methyl violet or Turk's solution, and cell quantification was performed with a Bürker chamber.

Flow cytometry of leukocytes in CSF, blood, and brain

Pups were killed with thiopental sodium, and blood was collected from the right ventricle and transferred to an EDTA-coated tube. RBCs were lysed by using RBC Lysis Buffer (Sigma-Aldrich, Stockholm, Sweden) before staining. CSF was collected as above, and for flow cytometry analysis at the 6-h time point, samples from 3 pups were pooled for each "n" as a result of the small volume of CSF. Leukocytes from blood and CSF were washed with PBS and pelleted by centrifugation at 400 *g* for 7 min at 4°C, then resuspended in PBS that contained 0.5% bovine serum albumin and FC Block (BD Pharmingen, Stockholm, Sweden) to block unspecific binding to FC receptors. Cells were stained with CD45 APC-Cy7 (Clone 30-F11; BD Pharmingen), CD11b FITC (Clone M1/70; eBiosciences, Stockholm, Sweden), Ly6C PE-Cy7 (Clone AL-21; BD Pharmingen), Ly6G PE (Clone 1A8; BD Pharmingen), TCRβ PE (Clone H57-597; eBiosciences), CD19 FITC (Clone 1D3; BD Pharmingen), and 7AAD (BD Pharmingen). Antibody amount was 0.2 μg per ~10^6 cells, and staining was performed at room temperature for 20 min. Flow cytometry was performed by using BD FACSCanto (BD Bioscience, Stockholm, Sweden). Gating strategy is shown in Fig. 2.

For flow cytometry of brain tissue, pups were killed 14 h after agonist administration by sodium thiopental overdose and perfused with saline for 2–3 min at a rate of 1 ml/min. Brains were cut into small pieces and washed with PBS to remove CSF residuals and then dissociated by using MACS Neural Tissue Dissociation Kit and gentleMACS Dissociator (Milteny Biotec, Lund, Sweden) following standard protocol. Single-cell suspensions were pelleted as above and resuspended in 30% Percoll solution (GE Healthcare, Pittsburgh, PA, USA), and added on top of a layer of 70% Percoll. Percoll gradients were centrifuged (950 *g*, 30 min, room temperature) and the enriched population of leukocytes/microglia was collected at the 70–30% Percoll interphase [18]. Enriched samples were then washed, blocked, and stained with CD45 APC-Cy7, CD11b FITC, and 7AAD for 30 min at 4°C. Single live cells were gated and analyzed for expression of CD45 and CD11b. Data were analyzed by using FlowJo (Tree Star, Ashland, OR, USA).

Immunohistochemistry

PND8 *Lys*-EGFP-*ki* mice were injected with P3C (5 mg/kg), LPS (0.3 mg/kg) or saline (0.9%). Pups were killed 14 h after injection and transcardially perfused with saline, followed by 4% paraformaldehyde. Brains were removed, postfixed in paraformaldehyde for 24 h at 4°C, and cryoprotected in 30% sucrose solution for at least 3 d. Cryoprotected brains were snap frozen on liquid nitrogen and serially sectioned at 40 μm on a Leica CM3050S cryostat (Leica, Wetzlar, Germany). Sections were stored in cryoprotectant solution (25% ethylene glycol, 25% glycerine, in 0.1 M phosphate buffer) at −20°C. Antigen retrieval was performed by 10 min incubation in 10 mM sodium citrate (pH6, at 97°C), and nonspecific binding sites were blocked by 30 min incubation in TBS that contained 3% donkey serum and 0.1% Triton X-100 (hereafter referred to as blocking buffer). Sections were then incubated overnight at 4°C in blocking buffer that contained Alexa Fluor 488–conjugated rabbit anti-GFP (1:200; Thermo Fisher Scientific), Mix-N-Stain CF657 (Sigma-Aldrich) conjugated goat polyclonal anti-CD31 (1:200; R&D Systems, Abingdon, United Kingdom), and rat monoclonal anti-Ly6G (1:250; clone 1A8; Biolegend, San Diego, CA, USA) before being incubated with donkey anti-rat CF555 (1:1000; VWR, Stockholm, Sweden) diluted in blocking buffer for 1 h at room temperature. Images were captured by using a Zeiss LSM 700 inverted confocal microscope equipped with Zen black software (Zeiss, Oberkochen, Germany).

Multiplex cytokine assay

PND8 mice were injected with P3C (1 or 5 mg/kg, i.p.), LPS (0.3 or 1 mg/kg, i.p.) or saline (0.9%, i.p.) and killed 6 h later. Blood was collected from the right ventricle of the heart and transferred to EDTA-coated tubes and spleens were dissected out. Animals were then transcardially perfused with saline and brains were removed. Spleen and brain tissue samples were frozen on dry ice immediately upon removal. Plasma was isolated from blood and frozen on dry ice. Brains and spleens were lysed by using a Bio-Plex Cell Lysis Kit (Bio-Rad, Hercules, CA, USA) plus ~~20%~~ 1 of 0.1 M PMSF (Sigma-Aldrich) on ice and by applying sonication (40% amplitude 18 pulses each 1.2 s, freeze and thaw, 10 pulses). Lysates were pelleted by centrifugation (4500 *g*, 5 min, 4°C) and stored at −80°C until use. Protein concentration was measured by using a Pierce BCA Protein Assay Kit (Thermo Fisher Scientific) following a standard protocol. Cytokine assay was performed by using a Bio-Plex Pro Mouse Cytokine Standard 23-Plex kit (Bio-Rad) following the manufacturer protocol, and cytokines were quantified on a Bio-Plex 200 Systems. Plasma samples were diluted 1:4 in diluent buffer, and brain and spleen samples were diluted 1:3 to load approximately 1–2 mg of protein. Obtained data were normalized to protein concentration and presented as Log10 of cytokine concentrations (picograms per milliliter for plasma samples and picograms per milligram protein for brain and spleen samples).

BBB and BCSFB permeability

Measurements of BBB and BCSFB permeability were performed as described recently [1]. In brief, 10 h after P3C (5 mg/kg), LPS (0.3 mg/kg), or saline injection, mice were injected intraperitoneally with [^{14}C]sucrose (0.2 μCi/g; American Radiolabeled Chemicals, St. Louis, MO, USA) and killed 30 min later with an overdose inhalation of isoflurane. Blood was collected from the heart and plasma was separated by centrifugation. CSF and different regions of brain were collected (cortex, striatum/thalamus, cerebellum, and

brainstem). All tissues and fluid samples were weighed. Radioactivity in samples was measured by liquid scintillation counting and calculated as cpm/mg. Tissue radioactivity was corrected for residual blood in tissues [8]. The concentration ratios between CSF/plasma and brain tissue/plasma were calculated as measures of BBB or BCSFB permeability.

Statistics

Data comparisons that involved >2 study groups (e.g., CSF leukocyte count, blood and brain flow cytometry, cytokine assay, and permeability test) were performed by 1-way ANOVA, followed by either Dunnett's or Tukey's post hoc tests. In Fig. 2H–J, comparisons between different doses of P3C were performed with Student's *t* test at each time point and corrected for multiple comparisons in accordance with the Holm-Sidak method. CSF leukocyte counts in adult TLR2 KO and MyD88 KO mice were compared by using Student's *t* test. Data are presented as means ± ~~SEM~~ SD unless otherwise stated. Statistical analysis was performed by using Prism V6.0 (GraphPad Software, La Jolla, CA, USA), and Radar charts were made by using Excel (Microsoft, Redmond, WA, USA).

RESULTS

P3C induces leukocyte infiltration into the CSF in a TLR2- and MyD88-dependent manner

Peripheral administration of low and high doses of P3C to neonatal mice induced substantial accumulation of leukocytes in the CSF, an effect detected as early as 6 h after injection (1 mg/kg: 418 ± 34 leukocytes/μl; $P < 0.05$; 5 mg/kg: 510 ± 111 leukocytes/μl; $P < 0.001$; compared with saline: 30 ± 15, n = 5–10/group; **Fig. 1A**), peaking at 14 h (1 mg/kg: 3508 ± 700 leukocytes/μl; $P < 0.001$; 5 mg/kg: 4378 ± 842 leukocytes/μl; $P < 0.0001$; compared with saline: 20 ± 9, n = 5–10/group; Fig. 1B), and still slightly increased at 48 h (1 mg/kg: 156 ± 32 leukocytes/μl; $P < 0.01$; 5 mg/kg: 153 ± 24 leukocytes/μl; $P < 0.001$; compared with saline: 12 ± 12, n = 5–10/group; Fig. 1D). In contrast, LPS at either low or high doses did not cause significant change in the number of leukocytes in CSF at 6, 14, or 24-h time points ($P > 0.05$; Fig. 1A–C); however, the high dose of LPS (1 mg/kg) caused a slight, but significant, elevation in CSF leukocyte count at the 48-h time point ($P < 0.05$; Fig. 1D). It is noteworthy that P3C caused similar effects in adult mice (1 mg/kg: 2963 ± 1290 leukocytes/μl vs. saline: 12 ± 7 leukocyte/μl at the 14-h time point; n = 3; P = 0.041). P3C injection in TLR2 KO and MyD88 KO neonatal mice did not result in significant changes in CSF leukocyte numbers at 14 h (TLR2 KO: 40 ± 20 leukocytes/μl; P = 0.24; ~~MyD88~~ 6 ± 2 leukocytes/μl; P = 0.31; compared with saline: 20 ± 9 leukocytes/μl; n = 3/group; Fig. 1B). To test the effect of other TLR2 heterodimers, the TLR2-TLR6 agonist FSL-1 was injected into neonatal mice. FSL-1 did not result in CSF pleocytosis at the 14-h time point (20 ± 20 leukocyte/μl vs. saline 20 ± 9 leukocytes/μl; P = 0.94; n = 3/group).

P3C-induced CSF infiltrating cells are mainly neutrophils and monocytes

We next sought to characterize CSF infiltrating leukocytes by flow cytometry. Cells were gated first on size and granularity (**Fig. 2A**),

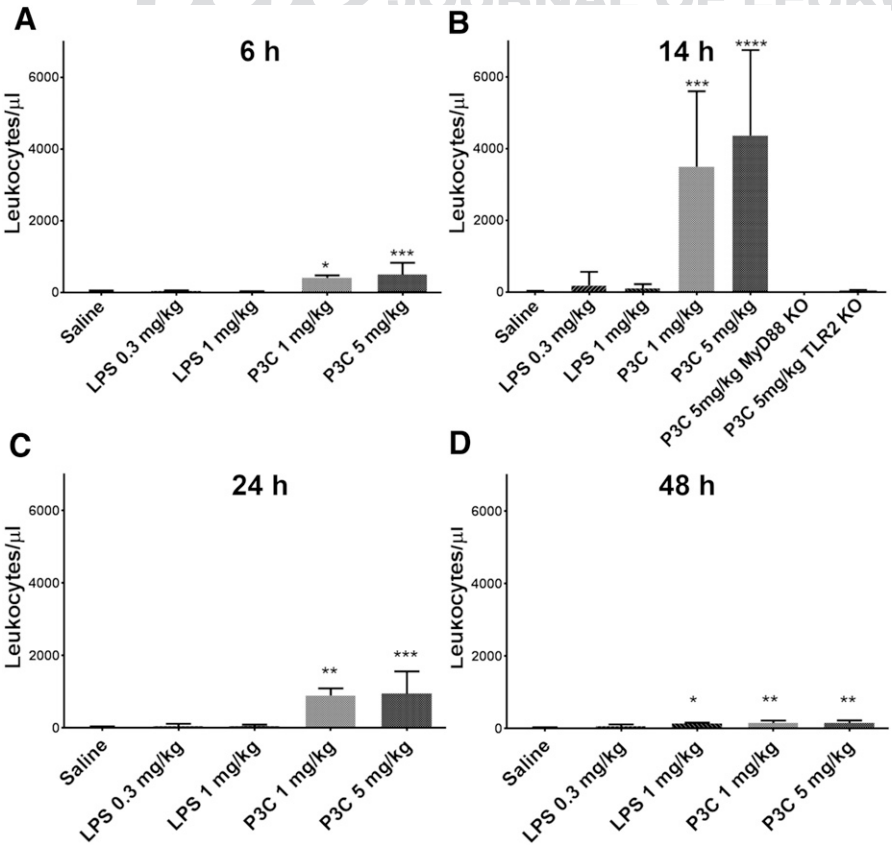

Figure 1. TLR1/2 activation induces infiltration of leukocytes into the CSF. (A–D) PND8 mice were injected with P3C (1 or 5 mg/kg, i.p.), LPS (0.3 or 1 mg/kg, i.p.), or saline, and leukocytes in the CSF were counted at 6 h (A), 14 h (B), 24 h (C), and 48 h (D). Data are presented as means ± SD. *$P \leq 0.05$; **$P \leq 0.01$; ***$P \leq 0.001$; ****$P \leq 0.0001$, 1-way ANOVA with Dunnett's post hoc test calculating the difference in relation to the saline group (n = 5–10/group).

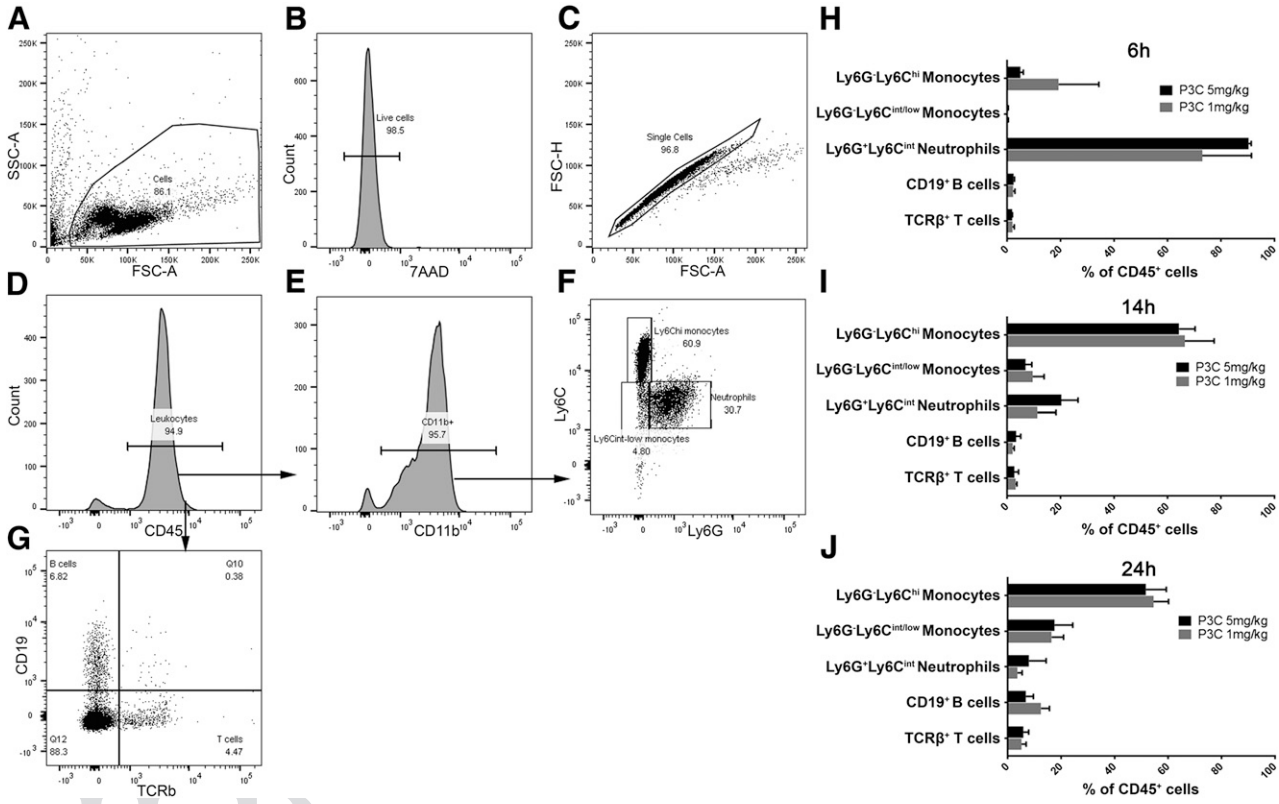

Figure 2. TLR2-induced CSF infiltrating cells are mainly neutrophils and inflammatory monocytes. PND8 mice were injected with P3C (1 or 5 mg/kg, i.p.), and CSF was collected for flow cytometry at 6, 14, or 24 h. (A–G) Representative images of flow cytometry gating strategy on CSF depicting cells in the CSF 14 h after injection of 5 mg/kg P3C. Live single cells were gated out and $CD45^+$ cells were further analyzed for expression of T cell (TCR-β^+) and B cell ($CD19^+$) markers, or gated for CD11b myeloid cells to be further analyzed for neutrophil ($Ly6G^+Ly6C^{int}$) and monocyte ($Ly6G^-Ly6C^{hi}$ or $Ly6G^-Ly6C^{low/int}$) markers. (H) CSF from 3 pups was pooled for each n at the 6-h time point ($n = 3$). (I and J) At 14 h (I) and 24 h (J), $Ly6C^{hi}$ inflammatory monocytes were the dominating cell population ($n = 7$–8). 7AAD = 7-aminoactinomycin D, FSC = forward scatter, SSC = side scatter. Data are presented as means ± SD.

followed by gating on live and single cells (Fig. 2B and C). Next, $CD45^+$ cells (Fig. 2D) were gated for expression of CD11b, followed by Ly6G and Ly6C to distinguish neutrophils and monocytes, respectively (Fig. 2E and F) [19]. $CD45^+$ cells were also gated for expression of TCR-β and CD19 to distinguish T cells and B cells, respectively (Fig. 2G). At 6 h after PC3 administration, the majority of $CD45^+$ leukocytes were $CD45^+CD11b^+Ly6G^+Ly6C^{int}$ neutrophils (1 mg/kg: 72.9 ± 9.2%; 5 mg/kg: 90.3 ± 7%; $n = 3$; Fig. 2H). At the 14-h time point, $CD45^+CD11b^+Ly6G^-Ly6C^{hi}$ monocytes were the dominating cell population in the CSF (1 mg/kg: 66.4 ± 4.4%; $n = 5$; 5 mg/kg: 64.3 ± 1.8%; $n = 10$; Fig. 2I). $Ly6G^-Ly6C^{hi}$ monocytes were the most prevalent cell population at the 24-h time point (1 mg/kg: 54.5%; $n = 7$; 5 mg/kg: 51.6 ± 2.7%; $n = 8$; Fig. 2J). No significant difference in CSF cell populations was observed between the 2 doses of P3C at any time point (Fig. 2H–J; $P > 0.05$).

P3C induces infiltration of leukocytes into the brain

To explore whether leukocytes are recruited to the brain after P3C or LPS administration, flow cytometry was performed on whole brain tissue. $CD11b^+CD45^{hi}$ cells were considered infiltrating leukocytes, whereas resident microglia were characterized as $CD11b^+CD45^{low}$ as previously described [20]. P3C administration resulted in a significantly higher proportion of $CD11b^+CD45^{hi}$ cells compared with control (P3C: 36 ± 5% vs. saline: 4.1 ± 0.5%; $P < 0.0001$; $n = 8$–10/group), which indicated increased infiltration of leukocytes into the brain (**Fig. 3A and B**). In contrast, there was no significant increase in the proportion of $CD11b^+CD45^{hi}$ cells in the brain after LPS administration (12.9 ± 1.8%; $P > 0.05$; $n = 8$; Fig. 3A and B).

To confirm flow cytometry results and explore the anatomic localization of CNS infiltrating leukocytes, we used *Lys*-EGFP-*ki* mice, a strain that expresses EGFP under the control of the LysM gene promoter, which is expressed in peripherally derived myeloid cells, including monocytes and neutrophils, but not in microglia [21]. In control animals (Fig. 3C–F), neutrophils ($EGFP^+Ly6G^+$) were not detected and the few observable $EGFP^+Ly6G^-$ cells, presumably monocytes, were localized within the lumen of $CD31^+$ blood vessels of meninges (Fig. 3D), periventricular regions (Fig. 3E), and the choroid plexus (Fig. 3F). LPS administration enhanced the presence of ($EGFP^+Ly6G^-$) monocytes and macrophages in the subarachnoid space (Fig. 3G), median eminence (Fig. 3H), periventricular endothelial cell layer (Fig. 3I), and the choroid plexus (Fig. 3J). These cells remained tightly associated with $CD31^+$ blood vessels but, in some

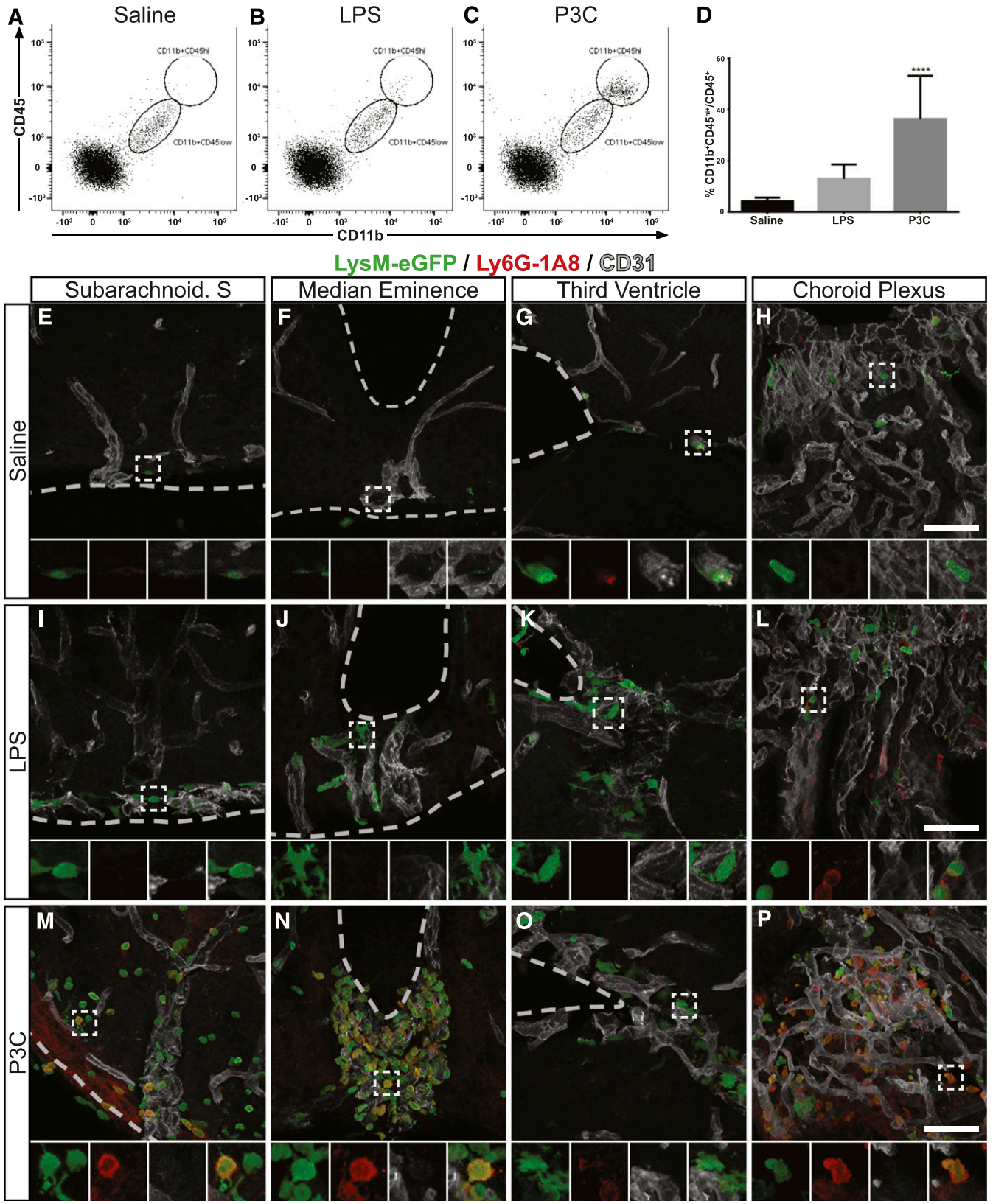

Figure 3. Leukocyte infiltration into the brain after peripheral administration of TLR1/2 agonist. PND8 mice injected with LPS (0.3 mg/kg, i.p.) or P3C (5 mg/kg i.p). Flow cytometry or immunohistochemistry was performed at 14 h. (A) Representative flow cytometry plot showing an increase in number of $CD11b^{+}CD45^{hi}$ infiltrating inflammatory leukocytes after P3C but not after LPS injection. (B) Quantification of flow cytometry data.

(*continued on next page*)

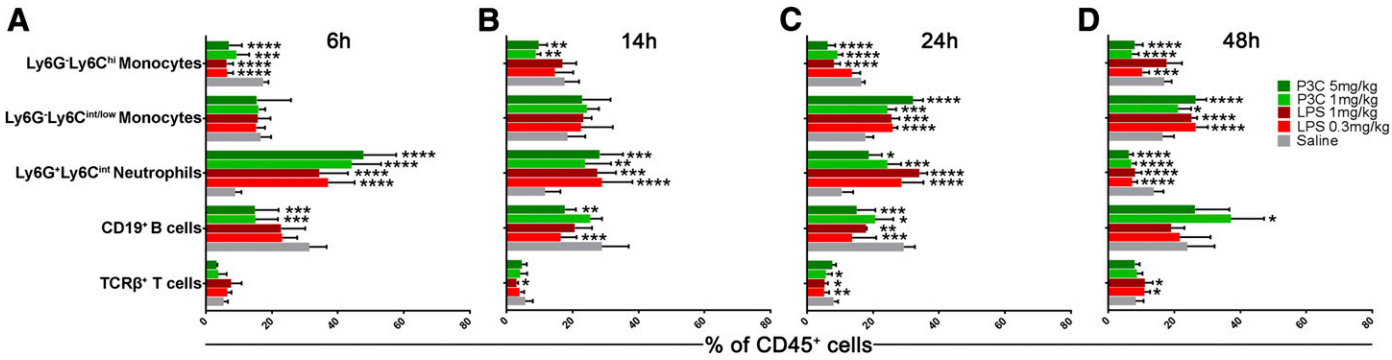

Figure 4. Cellular immune response in the circulation after P3C and LPS administration. PND8 mice were injected with P3C (1 or 5 mg/kg, i.p.), LPS (0.3 or 1 mg/kg, i.p.), or saline. (A–D) Blood was sampled at 6 (A), 14 (B), 24 (C), and 48 h (D), and cell populations were determined by flow cytometry. Gating strategies are as shown in Fig. 2. Data are presented as means ± SD. $*P \leq 0.05$; $**P \leq 0.01$; $***P \leq 0.001$; $****P \leq 0.0001$, 1-way ANOVA with Dunnett's post hoc test calculating the difference in relation to the saline group (n = 5–10).

cases, displayed the morphologic characteristics of perivascular macrophages and seemed to be localized outside the vessels (Fig. 3J, inset). LPS administration also resulted in the presence of neutrophils within the vasculature of the choroid plexus (Fig. 3J). P3C administration triggered a dramatic increase in neutrophils and macrophages within the subarachnoid space (Fig. 3K), median eminence (Fig. 3L), and the choroid plexus (Fig. 3N). Both neutrophils and macrophages could be observed in meningeal vessels (Fig. 3L) and within the CNS parenchyma (Fig. 3K and M). Accumulation of extravasated neutrophils and macrophages in the choroid plexus of P3C-treated animals was particularly striking (Fig. 3N). P3C did not induce $Ly6G^+$ neutrophil infiltration into the brain in TLR2 $^{-/-}$ mice (Supplemental Fig. S1).

P3C and LPS provoke similar cellular inflammatory response in circulation

To investigate the effect of TLR agonists on blood cellular composition, we performed flow cytometry on leukocytes from mice treated with different doses of P3C and LPS. Analysis of blood leukocytes revealed a relatively similar pattern of neutrophil response to both P3C and LPS. Between 6 and 24 h, both P3C and LPS induced an increase in neutrophils compared with saline-injected animals, followed by pronounced neutropenia at 48 h (**Fig. 4**). The proportion of $CD11b^+Ly6G^-Ly6C^{hi}$ monocytes was decreased by P3C compared with saline-injected pups at all time points studied. In contrast, LPS resulted in a more varied response in this population of monocytes, with no difference to control at the 14-h time point (Fig. 4). The proportion of $CD11b^+Ly6G^+Ly6C^{low/int}$ monocytes remained unaffected until 24 and 48 h after P3C or LPS administration, when there was a significant increase in the proportion of these cells (Fig. 4). The proportion of $CD19^+$ B cells generally decreased during the first 24 h after both P3C and LPS administration. A small population of TCR-β^+ T cells (<10% of $CD45^+$ cells) was detected in the blood. The response in these cells was varied, but seemed to be mostly reactive to LPS compared with P3C (Fig. 4).

P3C induces a distinct cytokine profile in the brain

To investigate the peripheral and CNS inflammatory responses, we performed 23-plex cytokine assays on plasma, spleen, and brain after treatment of neonatal mice with different doses of LPS and P3C. LPS, at both low and high doses, elicited the most potent peripheral cytokine response as measured in both plasma (**Fig. 5A**, Supplemental Table S1) and spleen (Fig. 5B, Supplemental Table S2). A more restricted response was noted in P3C-treated animals, where MCP-1, IL-12 (p40), IL-10, and IL-5 were increased in plasma compared with controls (Fig. 5A). In the spleen, MIP-1a, MCP-1, IL-12 (p40), IL-1a, IL-1b, and G-CSF were increased after P3C compared with saline (Fig. 5B). In the brain, 8 cytokines were increased after P3C compared with saline (MIP-1a, MIP-1b, MCP-1, ~~KC~~, IL-12p40, IL12p70, IL-1a, and G-CSF; Fig. 5C), whereas LPS triggered an increase in the release of 4 cytokines in the brain (RANTES, MCP-1, ~~KC~~, and G-CSF; Fig 5C, Supplemental Table S3). AQ:6

P3C increases the permeability of the BCSFB and BBB

To investigate whether P3C influences the properties of the BBB and BCSFB, we performed a sucrose permeability test at 10 h after P3C or LPS injection. Doses that caused the most similar patterns of peripheral inflammation were selected for the test, that is, 5 mg/kg P3C and 0.3 mg/kg LPS. P3C injections resulted in an increase of CSF/plasma ratios (P3C: 0.325 ± 0.015; compared with saline: 0.179 ± 0.010) and an increase in brain/plasma ratios across all brain areas (ratios increased 1.39–1.47 times across brain regions compared with controls), which was indicative of a particularly large increase in BCSFB permeability (**Fig. ~~6A~~**). In contrast, LPS injection resulted in no change in BCSFB or BBB permeability, nor did P3C significantly change barrier permeability in TLR2$^{-/-}$ mice (Supplemental Fig. S2).

(C–N) Representative confocal images of leukocytes in the subarachnoid spaces (C, G, K), median eminence (D, H, L), around the third ventricle (E, I, M), and the choroid plexus (F, J, N) of the brain 14 h after P3C injection. Green stain is LysM-expressing myeloid cells, red stain is $Ly6G^+$ neutrophils, and gray stain is $CD31^+$ endothelial cells. $****P \leq 0.0001$, 1-way ANOVA with Dunnett's post hoc test (n = 8–10/group).

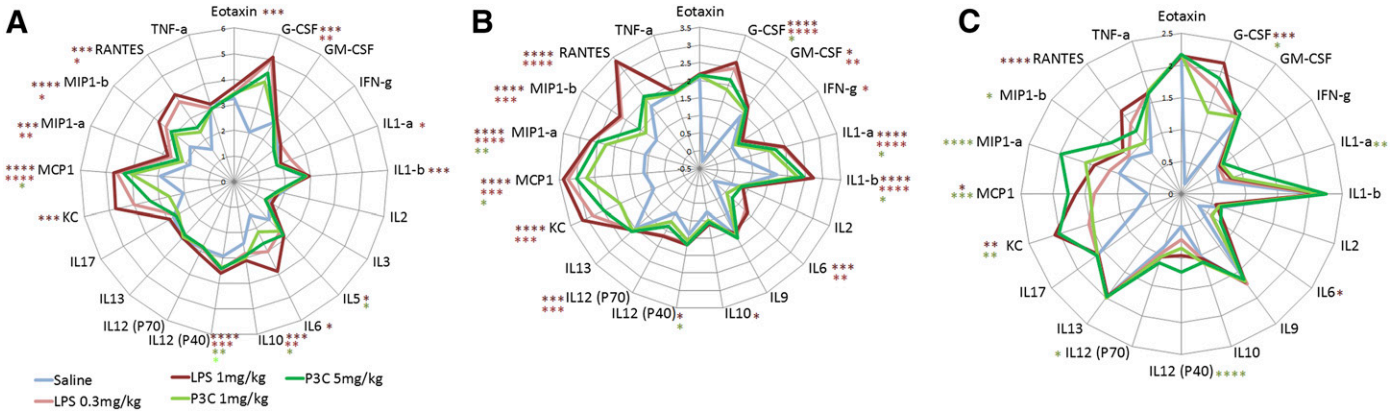

Figure 5. Peripheral and CNS cytokine responses by P3C and LPS. PND8 mice were injected with P3C (1 or 5 mg/kg, i.p.), LPS (0.3 or 1 mg/kg, i.p.), or saline. (A–C) Plasma (A), spleen (B), and brain (C) were collected 6 h after injection and analyzed by 23-plex cytokine assay. Radar charts show the Log10 of cytokine concentration (pg/ml for plasma samples and pg/mg protein for spleen and brain samples). KC = ~~XXXX~~. $^{*}P \leq 0.05$; $^{**}P \leq 0.01$; $^{***}P \leq 0.001$; $^{****}P \leq 0.0001$, 1-way ANOVA with Dunnett's post hoc test calculating the difference in relation to saline group ($n = 5$/group).

DISCUSSION

Inflammation in the newborn infant is a well-established risk factor for subsequent neurologic impairment, such as cerebral palsy [2, 4]. Leukocyte infiltration into the CSF is a clinical feature of meningitis or meningoencephalitis in newborns and adults [22, 23], and there is an association between neonatal meningitis and increased risk of cerebral palsy [24]. Sterile pleocytosis, that is, increased CSF leukocyte count without bacteria in the CSF, also occurs in newborn infants with, for example, urinary tract bacterial infection [25, 26]. However, it has been unclear how systemic bacterial infections are linked to inflammatory responses in the CSF and developing brain. Here, we present a pivotal pathway in which systemic activation of TLR2 results in increased permeability of the BCSFB and increased number of leukocytes in the CSF and brain concurrent with a heightened inflammatory response in the brain. We demonstrate that these effects are TLR2 and MyD88 dependent and not directly associated with overall peripheral inflammation. In addition, the strong proinflammatory TLR4 ligand, LPS, did not result in pleocytosis. Specific TLR2-mediated effects may be of importance for neurologic outcome in the newborn, as we have previously shown that repeated stimulation of TLR2 results in impaired brain development [14] and that the gram-positive bacteria *Staphylococcus epidermidis* induces brain injury in neonatal mice, partly via TLR2-dependent pathways [27]. Furthermore, TLR2-deficient mice are protected from neonatal hypoxia-ischemia, which further supports the importance of TLR2 in neonatal brain injury [13].

TLR2 is expressed on the cell surface where it forms heterodimers with either TLR1 or TLR6 [28]. Each heterodimer demonstrates different ligand specificity, with TLR1/TLR2 dimers binding bacterial triacylated lipopeptides, such as P3C, whereas TLR2/TLR6 dimers preferentially bind mycoplasmal diacylated lipoproteins, such as FSL-1 [29]. In the present study, FSL-1 did not cause leukocyte infiltration into the CSF, which suggests that the ~~TLR2-medicated~~ effect on pleocytosis is via the TLR1/TLR2 heterodimer.

Cellular composition of the CSF was characterized by an early dominance of neutrophils, followed by larger populations of $Ly6G^{-}Ly6C^{hi}$ monocytes at both 14 and 24 h and a minor increase in lymphocyte population at 24 h. This is in agreement with basic immunology dogma that neutrophils are the first to arrive at an inflammation site, followed by macrophages and lymphocytes [30]. $Ly6G^{-}Ly6C^{hi}$ monocytes constitute a small proportion of leukocytes in circulation and are rapidly recruited to infection/inflammation site [31]; therefore, the decrease in their frequency in circulation in response to P3C might be a result of their infiltration into the inflamed organs (e.g., the CNS), but also the incapability of bone marrow to completely reconstitute their population during the acute

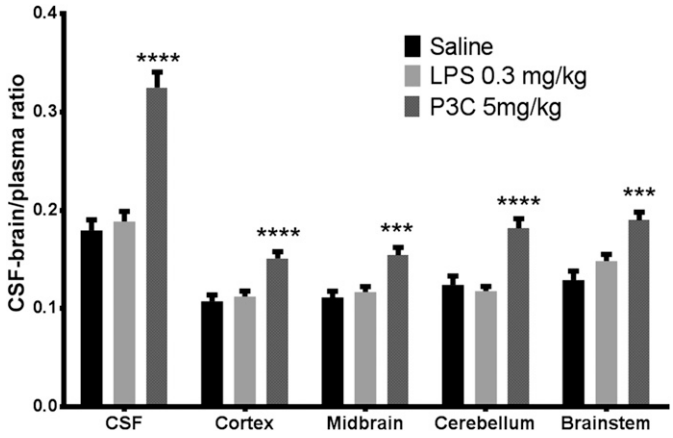

Figure 6. Increased permeability of BCSFB and BBB to sucrose after P3C administration. PND8 mice were injected with P3C (5 mg/kg, i.p.), LPS (0.3 mg/kg, i.p.), or saline. At 10 h after injection, the [^{14}C] sucrose permeability test was performed for CSF and different parts of the brain (cortex, striatum/thalamus, cerebellum, and brainstem). Data are presented as means ± SD. $^{***}P \leq 0.001$; $^{****}P \leq 0.0001$, 1-way ANOVA with Dunnett's post hoc test calculating the difference in relation to saline group ($n = 16$ for saline and P3C groups, and $n = 8$ for LPS group). Data are presented as means ± SD.

phase of inflammation [31]. In contrast, the proportion of $Ly6G^{-}Ly6C^{int/low}$ monocytes increased with time in circulation. This population of monocytes, also known as patrolling monocytes, crawls on endothelial cells in circulation, monitoring for infection/inflammation signals [32]. In patients with sepsis, $CD14^{dim}CD16^{+}$ monocytes—the homolog of mouse $Ly6G^{-}Ly6C^{int/low}$ monocytes—increase in number in circulation, and interestingly, express higher levels of TLR2 [33], which suggests a potential connection between TLR signaling and monocyte subset polarization.

The different effects of P3C and LPS on immune cells in the CSF and infiltrating cells in the brain are intriguing. Both TLR agonists induced a strong peripheral inflammation, which suggests that pleocytosis is not a common feature of systemic inflammation, but may be dependent on specific mechanisms in the BCSFB or BBB. Alternatively, cells in the CNS (e.g., microglia) may release specific chemoattractants in response to P3C that are different from LPS. In support of this, we found differences in the inflammatory response in the brain after P3C compared with LPS. In particular, MIP-1a (human synonym CCL3) emerged as the most differentially expressed cytokine in the brain after P3C injection compared with LPS. In support of this, in vitro data show that monocytic cells release more MIP-1a and for a longer time in response to P3C compared with LPS [34]. MIP-1a is known to have a role as a chemoattractant in recruiting monocytes and neutrophils to inflammation sites [35]. CCL3 is also detected in the CSF of individuals with bacterial meningitis [36] and its neutralization in experimental meningitis inhibits neutrophil recruitment to the CNS [37]. Expression of MIP-1a in the CNS could potentially attract cells and might, in part, explain the difference between P3C and LPS in causing infiltration of cells into the brain.

It should also be noted that one source of released cytokines can be the infiltrated cells themselves creating an inflammation-amplifying loop [38]. Although LPS caused release of RANTES and MCP-1 in the brain, this did not lead to significant leukocyte transmigration, which suggests that other factors than chemotaxis, for example, barrier structure remodeling, are required.

Infiltrating immune cells in brain tissue were localized to areas with close proximity to CSF-filled compartments, such as the circumventricular organs and the choroid plexus. The choroid plexus constitutes the BCSFB and could potentially play a role in cell infiltration into CSF. In support of this, we found that P3C induced a change in permeability, which was particularly prominent in this barrier. A similar effect was not observed after LPS, which indicated the BCSFB as a potentially major route of leukocyte entry after TLR2 activation. The difference in P3C and LPS effect is unlikely to be the result of different expressions of their corresponding receptors, as both TLR2 and TLR4 are known to be expressed in the choroid plexus [16, 39]. Whether the change in barrier properties is a result of the direct effect of P3C or secondary to transmigration of leukocytes warrants further investigation.

In summary, we report for the first time, to our knowledge, a TLR2-dependent leukocyte infiltration into the CSF and CNS of neonatal mice, largely through the BCSFB. Cell trafficking was not dependent on the degree of peripheral inflammation, as TLR4 activation by LPS did not result in significant cell infiltration despite eliciting a similar or higher inflammatory response in the circulation and spleen. The TLR2 agonist, P3C, induced release of chemokines, such as MIP-1a, in the brain that might be involved in recruiting leukocytes to the CNS. It also increased BCSFB permeability, which may facilitate leukocyte transmigration into the CSF. Altogether, this study describes an intriguing difference in TLR2- vs. TLR4-mediated inflammation on leukocyte trafficking into the immature brain.

AUTHORSHIP

A.M., C.J.E., and C.M. designed the experiments and analyzed the data. A.M., P.L.P.S., and C.J.E. performed the experiments. A.M. drafted the manuscript. H.H., C.J.E., and C.M. supervised the project. All authors contributed to the writing of the manuscript.

ACKNOWLEDGMENTS

This work was supported by the Swedish Research Council (2012-2992), a government grant in Public Health Service at the Sahlgrenska University Hospital (ALFGBG-142881), the Leducq Foundation (DSRR_P34404), the Swedish Brain Foundation (FO2014-008), Åhlén Foundation, and Torsten Söderberg Foundation (M98/15) to C.M. A.M. received grants from the Wilhelm and Martina Lundgren Foundation. The authors thank Anna-Lena Leverin and Pernilla Svedin for their excellent technical assistance.

Conflict of Interest Disclosure

The authors declare no conflicts of interest.

REFERENCES

1. Grether, J. K., Nelson, K. B. (1997) Maternal infection and cerebral palsy in infants of normal birth weight. *JAMA* **278,** 207–211.
2. Strunk, T., Inder, T., Wang, X., Burgner, D., Mallard, C., Levy, O. (2014) Infection-induced inflammation and cerebral injury in preterm infants. *Lancet Infect. Dis.* **14,** 751–762.
3. Sävman, K., Blennow, M., Gustafson, K., Tarkowski, E., Hagberg, H. (1998) Cytokine response in cerebrospinal fluid after birth asphyxia. *Pediatr. Res.* **43,** 746–751.
4. Hagberg, H., Mallard, C., Ferriero, D. M., Vannucci, S. J., Levison, S. W., Vexler, Z. S., Gressens, P. (2015) The role of inflammation in perinatal brain injury. *Nat. Rev. Neurol.* **11,** 192–208.
5. Shechter, R., London, A., Schwartz, M. (2013) Orchestrated leukocyte recruitment to immune-privileged sites: absolute barriers versus educational gates. *Nat. Rev. Immunol.* **13,** 206–218.
6. Johansson, P. A., Dziegielewska, K. M., Liddelow, S. A., Saunders, N. R. (2008) The blood-CSF barrier explained: when development is not immaturity. *BioEssays* **30,** 237–248.
7. Ek, C. J., Dziegielewska, K. M., Habgood, M. D., Saunders, N. R. (2012) Barriers in the developing brain and neurotoxicology. *Neurotoxicology* **33,** 586–604.
8. Ek, C. J., D'Angelo, B., Baburamani, A. A., Lehner, C., Leverin, A. L., Smith, P. L., Nilsson, H., Svedin, P., Hagberg, H., Mallard, C. (2015) Brain barrier properties and cerebral blood flow in neonatal mice exposed to cerebral hypoxia-ischemia. *J. Cereb. Blood Flow Metab.* **35,** 818–827.
9. Rosenberg, G. A. (2012) Neurological diseases in relation to the blood-brain barrier. *J. Cereb. Blood Flow Metab.* **32,** 1139–1151.
10. Akira, S., Uematsu, S., Takeuchi, O. (2006) Pathogen recognition and innate immunity. *Cell* **124,** 783–801.
11. Eklind, S., Mallard, C., Leverin, A.-L., Gilland, E., Blomgren, K., Mattsby-Baltzer, I., Hagberg, H. (2001) Bacterial endotoxin sensitizes the

immature brain to hypoxic–ischaemic injury. *Eur. J. Neurosci.* **13,** 1101–1106.
12. Stridh, L., Mottahedin, A., Johansson, M. E., Valdez, R. C., Northington, F., Wang, X., Mallard, C. (2013) Toll-like receptor-3 activation increases the vulnerability of the neonatal brain to hypoxia-ischemia. *J. Neurosci.* **33,** 12041–12051.
13. Stridh, L., Smith, P. L., Naylor, A. S., Wang, X., Mallard, C. (2011) Regulation of toll-like receptor 1 and -2 in neonatal mice brains after hypoxia-ischemia. *J. Neuroinflammation* **8,** 45.
14. Du, X., Fleiss, B., Li, H., D'angelo, B., Sun, Y., Zhu, C., Hagberg, H., Levy, O., Mallard, C., Wang, X. (2011) Systemic stimulation of TLR2 impairs neonatal mouse brain development. *PLoS One* **6,** e19583.
15. Hoffmann, O., Braun, J. S., Becker, D., Halle, A., Freyer, D., Dagand, E., Lehnardt, S., Weber, J. R. (2007) TLR2 mediates neuroinflammation and neuronal damage. *J. Immunol.* **178,** 6476–6481.
16. Stridh, L., Ek, C. J., Wang, X., Nilsson, H., Mallard, C. (2013) Regulation of Toll-like receptors in the choroid plexus in the immature brain after systemic inflammatory stimuli. *Transl. Stroke Res.* **4,** 220–227.
17. Hübschle, T., Mütze, J., Mühlradt, P. F., Korte, S., Gerstberger, R., Roth, J. (2006) Pyrexia, anorexia, adipsia, and depressed motor activity in rats during systemic inflammation induced by the Toll-like receptors-2 and -6 agonists MALP-2 and FSL-1. *Am. J. Physiol. Regul. Integr. Comp. Physiol.* **290,** R180–R187.
18. Roussarie, J. P., Ruffié, C., Brahic, M. (2007) The role of myelin in Theiler's virus persistence in the central nervous system. *PLoS Pathog.* **3,** e23.
19. Rose, S., Misharin, A., Perlman, H. (2012) A novel Ly6C/Ly6G-based strategy to analyze the mouse splenic myeloid compartment. *Cytometry A* **81,** 343–350.
20. Denker, S. P., Ji, S., Dingman, A., Lee, S. Y., Derugin, N., Wendland, M. F., Vexler, Z. S. (2007) Macrophages are comprised of resident brain microglia not infiltrating peripheral monocytes acutely after neonatal stroke. *J. Neurochem.* **100,** 893–904.
21. Faust, N., Varas, F., Kelly, L. M., Heck, S., Graf, T. (2000) Insertion of enhanced green fluorescent protein into the lysozyme gene creates mice with green fluorescent granulocytes and macrophages. *Blood* **96,** 719–726.
22. van de Beek, D., de Gans, J., Tunkel, A. R., Wijdicks, E. F. M. (2006) Community-acquired bacterial meningitis in adults. *N. Engl. J. Med.* **354,** 44–53.
23. Kim, K. S. (2010) Acute bacterial meningitis in infants and children. *Lancet Infect. Dis.* **10,** 32–42.
24. Kułak, W., Okurowska-Zawada, B., Sienkiewicz, D., Paszko-Patej, G., Krajewska-Kułak, E. (2010) Risk factors for cerebral palsy in term birth infants. *Adv. Med. Sci.* **55,** 216–221.
25. Syrogiannopoulos, G. A., Grivea, I. N., Anastassiou, E. D., Triga, M. G., Dimitracopoulos, G. O., Beratis, N. G. (2001) Sterile cerebrospinal fluid pleocytosis in young infants with urinary tract infection. *Pediatr. Infect. Dis. J.* **20,** 927–930.
26. Doby, E. H., Stockmann, C., Korgenski, E. K., Blaschke, A. J., Byington, C. L. (2013) Cerebrospinal fluid pleocytosis in febrile infants 1-90 days with urinary tract infection. *Pediatr. Infect. Dis. J.* **32,** 1024–1026.
27. Bi, D., Qiao, L., Bergelson, I., Ek, C. J., Duan, L., Zhang, X., Albertsson, A. M., Pettengill, M., Kronforst, K., Ninkovic, J., Goldmann, D., Janzon, A., Hagberg, H., Wang, X., Mallard, C., Levy, O. (2015) *Staphylococcus epidermidis* bacteremia induces brain injury in neonatal mice via Toll-like receptor 2-dependent and -independent pathways. *J. Infect. Dis.* **212,** 1480–1490.
28. Jin, M. S., Kim, S. E., Heo, J. Y., Lee, M. E., Kim, H. M., Paik, S. G., Lee, H., Lee, J. O. (2007) Crystal structure of the TLR1-TLR2 heterodimer induced by binding of a tri-acylated lipopeptide. *Cell* **130,** 1071–1082.
29. Morr, M., Takeuchi, O., Akira, S., Simon, M. M., Mühlradt, P. F. (2002) Differential recognition of structural details of bacterial lipopeptides by Toll-like receptors. *Eur. J. Immunol.* **32,** 3337–3347.
30. Medzhitov, R. (2008) Origin and physiological roles of inflammation. *Nature* **454,** 428–435.
31. Serbina, N. V., Pamer, E. G. (2006) Monocyte emigration from bone marrow during bacterial infection requires signals mediated by chemokine receptor CCR2. *Nat. Immunol.* **7,** 311–317.
32. Auffray, C., Fogg, D., Garfa, M., Elain, G., Join-Lambert, O., Kayal, S., Sarnacki, S., Cumano, A., Lauvau, G., Geissmann, F. (2007) Monitoring of blood vessels and tissues by a population of monocytes with patrolling behavior. *Science* **317,** 666–670.
33. Cros, J., Cagnard, N., Woollard, K., Patey, N., Zhang, S.-Y., Senechal, B., Puel, A., Biswas, S. K., Moshous, D., Picard, C., Jais, J.-P., D'Cruz, D., Casanova, J.-L., Trouillet, C., Geissmann, F. (2010) Human CD14dim monocytes patrol and sense nucleic acids and viruses via TLR7 and TLR8 receptors. *Immunity* **33,** 375–386.
34. Parker, L. C., Whyte, M. K. B., Vogel, S. N., Dower, S. K., Sabroe, I. (2004) Toll-like receptor (TLR)2 and TLR4 agonists regulate CCR expression in human monocytic cells. *J. Immunol.* **172,** 4977–4986.
35. Reichel, C. A., Puhr-Westerheide, D., Zuchtriegel, G., Uhl, B., Berberich, N., Zahler, S., Wymann, M. P., Luckow, B., Krombach, F. (2012) C-C motif chemokine CCL3 and canonical neutrophil attractants promote neutrophil extravasation through common and distinct mechanisms. *Blood* **120,** 880–890.
36. Spanaus, K. S., Nadal, D., Pfister, H. W., Seebach, J., Widmer, U., Frei, K., Gloor, S., Fontana, A. (1997) C-X-C and C-C chemokines are expressed in the cerebrospinal fluid in bacterial meningitis and mediate chemotactic activity on peripheral blood-derived polymorphonuclear and mononuclear cells in vitro. *J. Immunol.* **158,** 1956–1964.
37. Diab, A., Abdalla, H., Li, H. L., Shi, F. D., Zhu, J., Höjberg, B., Lindquist, L., Wretlind, B., Bakhiet, M., Link, H. (1999) Neutralization of macrophage inflammatory protein 2 (MIP-2) and MIP-1α attenuates neutrophil recruitment in the central nervous system during experimental bacterial meningitis. *Infect. Immun.* **67,** 2590–2601.
38. Silva, M. T. (2010) When two is better than one: macrophages and neutrophils work in concert in innate immunity as complementary and cooperative partners of a myeloid phagocyte system. *J. Leukoc. Biol.* **87,** 93–106.
39. Rivest, S. (2009) Regulation of innate immune responses in the brain. *Nat. Rev. Immunol.* **9,** 429–439. **AQ:8**

KEY WORDS:
BBB · BCSFB · meningitis · PAM3CSK4 · inflammation · pleocytosis